Supporting Information (SI) for

Hybrid Membranes of Zeolitic Imidazolate Frameworks with Cage-like Pores for Solar Steam Evaporation

Yingying Zhu[a,‡], Hongyu Lan[a,‡], Panpan He[b], Xiangwei Zhu[d], Jiang Gong[b], Zhiyue Dong[a,], Minghua Zeng[a,c,*]*

[a] Hubei Collaborative Innovation Center for Advanced Chemical Materials, Ministry of Education Key Laboratory for the Synthesis and Application of Organic Functional Molecules and College of Chemistry and Chemical Engineering, Hubei University, Wuhan 430062, China.

[b] Key Laboratory of Material Chemistry for Energy Conversion and Storage, Ministry of Education, Hubei Key Laboratory of Material Chemistry and Service Failure, School of Chemistry and Chemical Engineering, Huazhong University of Science and Technology, Wuhan 430074, China.

[c] School of Chemistry and Pharmaceutical Sciences Guangxi Normal University, Key Laboratory for the Chemistry and Molecular Engineering of Medicinal Resources Guilin, 541004, China.

[d] National "111" Center for Cellular Regulation and Molecular Pharmaceutics, Key Laboratory of Fermentation Engineering (Ministry of Education), Hubei Key Laboratory of Industrial Microbiology, Hubei University of Technology, Wuhan, 430068, China.

*Correspondence authors.

mail addresses: dzhyue@hubu.edu.cn (Z.D.); zmh@mailbox.gxnu.edu.cn (M.Z.).

‡ These authors contributed equally.

Contents in SI

Section S1	Measurement of ZCP-x membranes Materials	**S3**
Section S2	Characterization of ZCP-x membrane	**S3-S9**
Reference in SI		**S9-S12**

Section S1: **Measurement of ZCP-x membranes Materials Characterization**

Powder X-ray diffraction (PXRD) was performed on a Rigaku Smartlab 9 kW X-ray diffractometer at room temperature, in parallel beam geometry employing Cu Kα lines focused radiation at 9 kW (45 kV, 200 mA) power. The morphology was observed by means of a field-emission scanning electron microscope (SEM, Sigma500) with the accelerating voltage of 5 kV. The distribution of surface element was analyzed using an energy dispersive X-ray spectrometer (EDX, Genesis 2000). Fourier-transform infrared spectroscopy (FT-IR) was performed in Bruker VERTEX 70 at room temperature. The sample was mixed with KBr at the weight ratio of 1:150. N_2 adsorption/desorption experiments were executed on the Micromeritics ASAP 2460 under a liquid nitrogen bath (77 K). The contact angle was executed on interface viscoelastic measuring device (Dataphysics, 0CA15EC). The absorption spectrum was tested using a UV-Vis-NIR spectrophotometer (Lambda 750S) with an integrating sphere. Optical images were got by Mshot MS60 optical microscope.

Section S2: **Characterization of ZCP-x membrane**

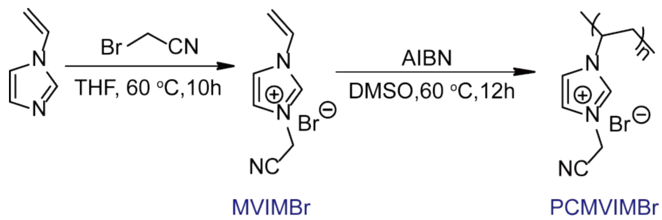

Figure S1 Synthetic route of PCMVIMBr.

Table S1 Mass ratio of different parts in ZCP-x (ZIF-8 : CNT : PCMVIMBr = 10 : n : 3.4) membranes. x stands for the mass ratio of CNTs in the hybrid membranes.

Sample name (ZCP-x)	ZIF-8	CNT (n)	PCMVIMBr
ZCP-0	10	0	3.4
ZCP-5	10	0.705	3.4
ZCP-10	10	1.489	3.4
ZCP-15	10	2.010	3.4
ZCP-20	10	3.350	3.4
ZCP-25	10	4.467	3.4
ZCP-30	10	5.743	3.4

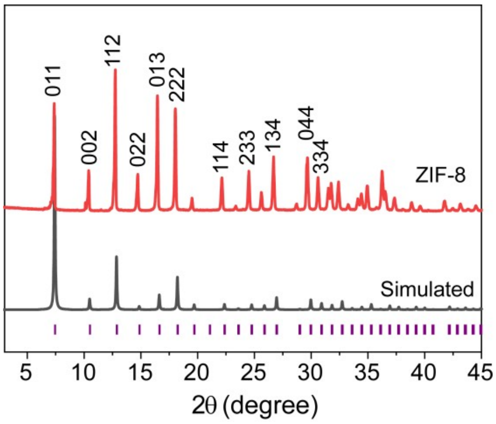

Figure S2 PXRD pattern of ZIF-8.

Please note: the diffraction peaks of ZIF-8 match well with the simulated pattern.

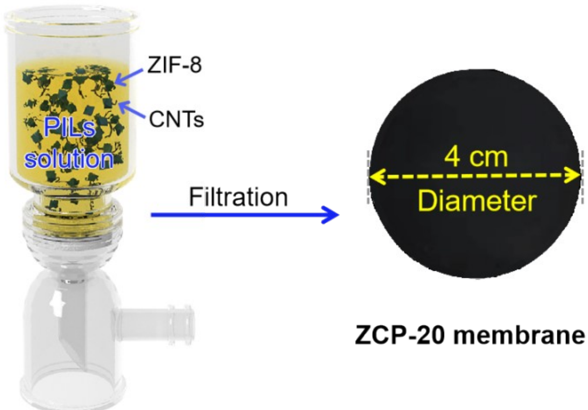

Figure S3 Picture of ZCP-20 membrane and its dimensions.

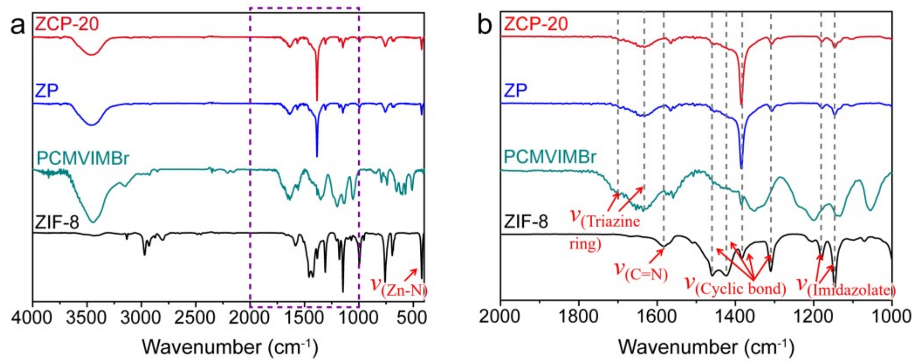

Figure S4 FT-IR curves of different membranes (a) the complete and (b) enlarged curve.

Please note: New FT-IR bands at 1695 cm^{-1} and 1635 cm^{-1} were observed in the NH_3-treated PCMVImBr nanomembrane and were absent in the non-treated PCMVImBr. These peaks are consistent with the ν (C=N) and ν (C-N) IR bands reported for triazine rings.[1]

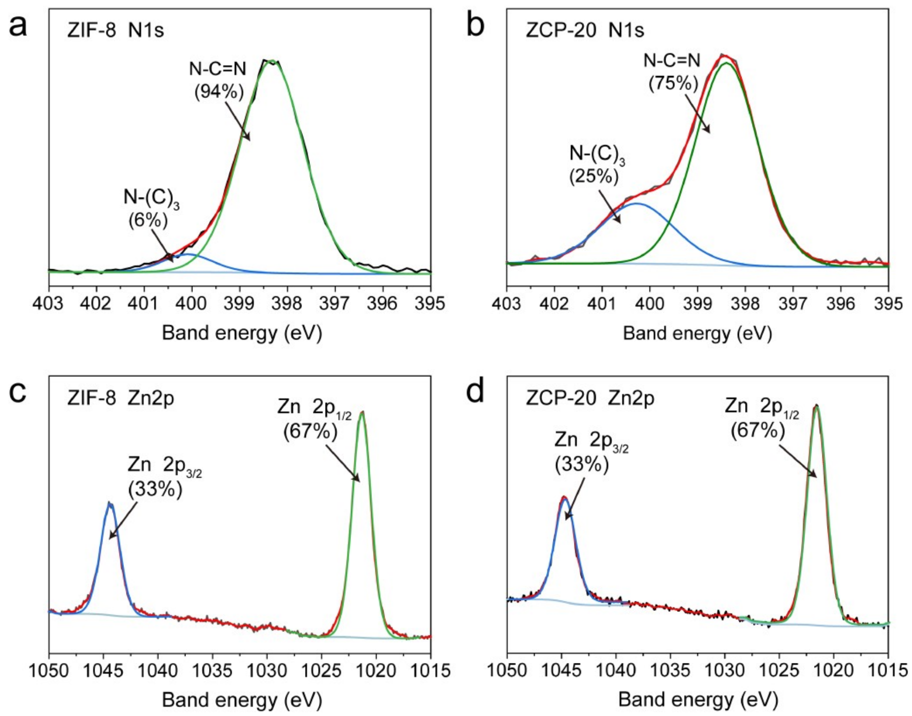

Figure S5 High-resolution N1s XPS spectra of (a) ZIF-8, (b) ZCP-20, and Zn 2p XPS spectra of (c) ZIF-8 and (d) ZCP-20.

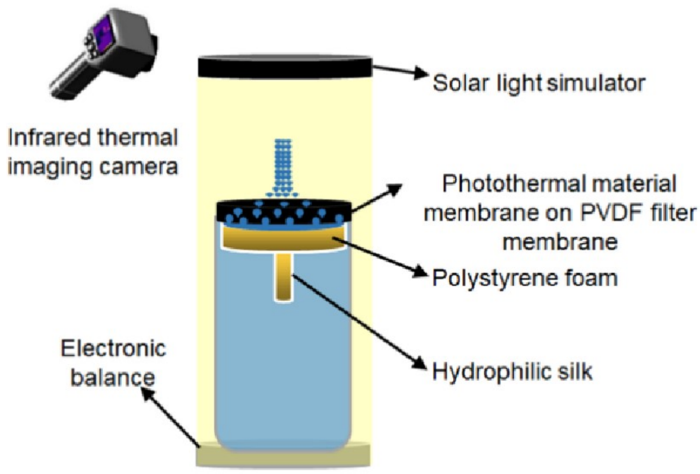

Figure S6 Schematic illustration of the solar steam generation instrument used in this work.

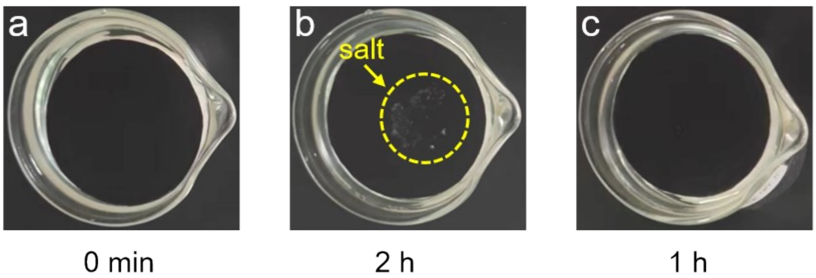

Figure S7 Water evaporation tests of ZCP-20 membrane for seawater. Please note: there are some crystals on the surface of ZCP-20 membrane after 2 hours under 1 sunlight irradiation (b) and the salt crystals are dissolved within1 hour in dark (c).

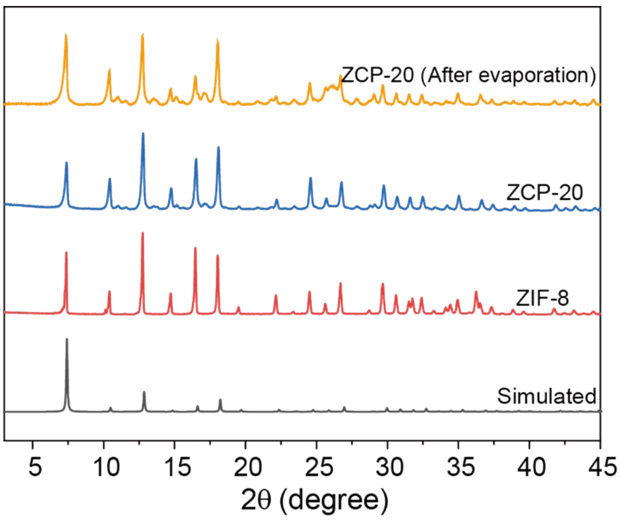

Figure S8 PXRD curves of ZIF-8, ZCP-20, ZCP-20 (After evaporation).

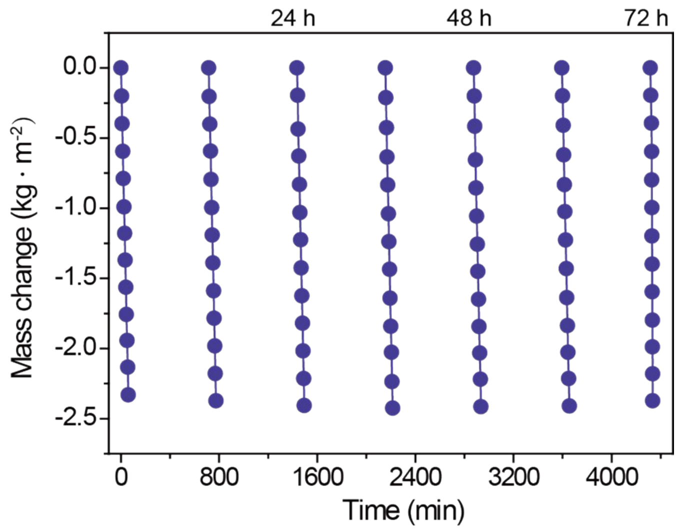

Figure S9 Recyclability of ZCP-20 (every interval 12 hours for 3 days).

Table S2 Comparison of ZCP-20 membrane with previously reported materials in interfacial solar vapor generation.

	Photothermal material	Evaporation rate (kg/m^2/h)	Efficiency (%)	Reference in ESI	Metal	Remarks
1	ZCP-20	2.48	67.1	This work	Metal free	Open system
2	Ppy@Co_3O_4 @Al sheet	1.94	84.7	2	Metal	Closed system
3	p-Magnetic carbon (p-MC)	1.46	70.3	3	Metal	Open system
4	CNTs@melamine/silicone sponges (CNTs@MS)	1.75	77.4	4	Metal free	Open system
5	NiS_2@Ti_3C_2	1.27	83.84	5	Metal	Open system
6	1T/2H FMoS_2	1.52	90	6	Metal	Open system
7	CNT-CNF	1.41	96.8	7	Metal free	Open system

8	Co-Zn ZIF/MoS_2 hybrid nanosheets	1.394	85.3	8	Metal	Open system
9	Cu@C/CLS	1.54	90.2	9	Metal	Open system
10	CBC-500	1.97	64.42	10	Metal	Open system
11	Fe_2O_3/CNT/NF NanocompositeFoam	1.48	81.3	11	Metal	Open system
12	G@ZIF	1.78	96	12	Metal	Open system
13	rGO-SA aerogels	1.86	89.38	13	Metal free	Open system
14	GO-HNT	1.61	83.67	14	Metal free	Open system
15	MnO/C	2.38	98.4	15	Metal	Open system
16	MoCOF@Gel	2.31	91.8	16	Metal	Open system
17	NRGO	2.8	87	17	Metal free	Open system
18	G-CNF/PI/CNT	1.58	80.1	18	Metal free	Open system
19	Chitosan/PNAGA-CNTs	2.42	92	19	Metal free	Open system
20	TA@APTES@Fe^{3+}	1.8	87	20	Metal	Open system
21	MOF-801@carbonized loofah	1.42	88.9	21	Metal	Open system
22	Zr–Fc MOF/SWCNT/gelatin, ZSG	1.53	95.6	22	Metal	Open system
23	Cu-MOF photothermal textile	1.52	88	23	Metal	Open system

24	Co_3S_4HP/PAN	1.26	86.5	24	Metal	Open system
25	Wood/ZIF-8/PDA	2.7	86	25	Metal	Open system
26	PCG membrane	2.07	80.2	26	Metal	Open system
27	Ag-Cu/SDB@PVA membrane	1.49	90.4	27	Metal	Open system
28	VA-GSM	1.62	86.5	28	Metal free	Open system
29	Ag-PSS-AG/AG device	2.1	92.8	29	Metal	Open system
30	GO-based aerogel	2.89	66.9	30	Metal free	Open system

Reference in SI

[1] Täuber, K.; Dani, A.; Yuan, J., Covalent Cross-Linking of Porous Poly(ionic liquid) Membrane via a Triazine Network. *ACS Macro Letters.*, **2016**, *6*, 1-5.

[2] Chen, K.; Li, L.; Zhang, J., Design of a Separated Solar Interfacial Evaporation System for Simultaneous Water and Salt Collection. *ACS Appl. Mater. Interfaces.,* **2021**, *13*, 59518-59526.

[3] Li, L.; Hu, T.; Li, A.; Zhang, J., Electrically Conductive Carbon Aerogels with High Salt-Resistance for Efficient Solar-Driven Interfacial Evaporation. *ACS Appl. Mater. Interfaces.,* **2020**, *12*, 32143-32153.

[4] Li, L.; Li, Q.; Feng, Y.; Chen, K.; Zhang, J., Melamine/Silicone Hybrid Sponges with Controllable Microstructure and Wettability for Efficient Solar-Driven Interfacial Desalination. *ACS Appl. Mater. Interfaces.,* **2022**, *14*, 2360-2368.

[5] Wang, Z.; Xu, W.; Yu, K.; Gong, S.; Mao, H.; Huang, R.; Zhu, Z., NiS2 Nanocubes Coated Ti3C2 Nanosheets with Enhanced Light-to-Heat Conversion for Fast and Efficient Solar Seawater Steam Generation. *Sol. RRL.,* **2021**, *5*, 2100183.

[6] Guo, Z. Z.; Chen, Z. H.; Shi, Z. X.; Qian, J. W.; Li, J. H.; Mei, T.; Wang, J. Y.; Wang, X. B.; Shen, P., Stable metallic 1T phase engineering of molybdenum disulfide for enhanced solar vapor generation. *Sol. Energy Mater. Sol. Cells.,* **2020**, *204*, 110227.
[7] Li, K.; Gao, M.; Li, Z.; Yang, H.; Jing, L.; Tian, X.; Li, Y.; Li, S.; Li, H.; Wang, Q.; Ho, J. S.; Ho, G. W.; Chen, P.-Y., Multi-interface engineering of solar evaporation devices via scalable, synchronous thermal shrinkage and foaming. *Nano Energy.,* **2020**, *74*, 104875.
[8] Peng, H.; Zhang, L.; Li, M.; Liu, M.; Wang, C.; Wang, D.; Fu, S., Interfacial growth of 2D bimetallic metal-organic frameworks on MoS2 nanosheet for reinforcements of polyacrylonitrile fiber: From efficient flame-retardant fiber to recyclable photothermal materials. *Chem. Eng. J,* **2020**, *397*, 125410.
[9] Ren, L.; Yi, X.; Yang, Z.; Wang, D.; Liu, L.; Ye, J., Designing Carbonized Loofah Sponge Architectures with Plasmonic Cu Nanoparticles Encapsulated in Graphitic Layers for Highly Efficient Solar Vapor Generation. *Nano letters.,* **2021**, *21*, 1709-1715.
[10] Chen, G.; Jiang, Z.; Li, A.; Chen, X.; Ma, Z.; Song, H., Cu-based MOF-derived porous carbon with highly efficient photothermal conversion performance for solar steam evaporation. *J. Mater. Chem. A,* **2021**, *9*, 16805-16813.
[11] Shuang Han, J. Y., Xiaofeng Li, Wei Li, Xintao Zhang, Nikhil Koratkar, Zhong-Zhen Yu, Flame Synthesis of Superhydrophilic Carbon Nanotubes-Ni Foam Decorated with Fe2O3 Nanoparticles. *ACS Appl. Mater. Interfaces.,* **2020**, *12*, 13239-13238.
[12] Han, X.; Besteiro, L. V.; Koh, C. S. L.; Lee, H. K.; Phang, I. Y.; Phan-Quang, G. C.; Ng, J. Y.; Sim, H. Y. F.; Lay, C. L.; Govorov, A.; Ling, X. Y., Intensifying Heat Using MOF-Isolated Graphene for Solar-Driven Seawater Desalination at 98% Solar to Thermal Efficiency. *Adv. Funct. Mater.,* **2021**, *31*, 2008904.
[13] Jian, H.; Wang, Y.; Li, W.; Ma, Y.; Wang, W.; Yu, D., Reduced graphene oxide aerogel with the dual-cross-linked framework for efficient solar steam evaporation. *Colloids and Surfaces A: Physicochemical and Engineering Aspects.,* **2021**, *629*, 127440.

[14] Xia, M.; Chen, L.; Zhang, C.; Hasi, Q.-M.; Li, Z.; Li, H., Porous architectures based on halloysite nanotubes as photothermal materials for efficient solar steam generation. *Appl. Clay Sci.,* **2020**, *189*, 105523.

[15] Fan, Z.; Ren, J.; Bai, H.; He, P.; Hao, L.; Liu, N.; Chen, B.; Niu, R.; Gong, J., Shape-controlled fabrication of MnO/C hybrid nanoparticle from waste polyester for solar evaporation and thermoelectricity generation. *Chem. Eng. J,* **2023**, *451*, 138534.

[16] Xia, M.; Liang, Y.; Luo, W.; Cai, D.; Zhao, P.; Chen, F.; Li, Y.; Sui, Z.; Shan, L.; Fan, R.; Pan, F.; Wang, D.; Li, M.; Shen, Y.; Xiao, J.; Wu, X.; Chen, Q., 2D covalent organic framework-based core-shell structures for high-performance solar-driven steam generation. *Mater. Today Energy.,* **2022**, *29*, 101135.

[17] Chen, Y.; Sha, C.; Wang, W.; Yang, F., Solar-driven steam generation on nitrogen-doped graphene in a 2D water path isolation system. *Mater. Res. Exps.,* **2020**, *7*, 015507.

[18] Lan, K.; Deng, Y.; Huang, A.; Li, S.-Q.; Liu, G.; Xie, H.-L., Highly-performance polyimide as an efficient photothermal material for solar-driven water evaporation. *Polymer.,* **2022**, *256*, 125177.

[19] Lu, H.; Li, M.; Wang, X.; Wang, Z.; Pi, M.; Cui, W.; Ran, R., Recyclable physical hydrogels as durable and efficient solar-driven evaporators. *Chem. Eng. J,* **2022**, *450*, 138257.

[20] Wang, Z.; Han, M.; He, F.; Peng, S.; Darling, S. B.; Li, Y., Versatile coating with multifunctional performance for solar steam generation. *Nano Energy.,* **2020**, *74*, 104886.

[21] Guo, M. X.; Wu, J. B.; Zhao, H. Y.; Li, F. H.; Min, F. Q., Carbonized loofah and MOF-801 of synergistic effect for efficient solar steam generation. *Int. J. Energy Res.,* **2021**, *45*, 10599-10608.

[22] Ma, X.; Deng, Z.; Li, Z.; Chen, D.; Wan, X.; Wang, X.; Peng, X., A photothermal and Fenton active MOF-based membrane for high-efficiency solar water evaporation and clean water production. *J. Mater. Chem. A,* **2020**, *8*, 22728-22735.

[23] Wang, J.; Wang, W.; Feng, L.; Yang, J.; Li, W.; Shi, J.; Lei, T.; Wang, C., A salt-

free superhydrophilic metal-organic framework photothermal textile for portable and efficient solar evaporator. *Sol. Energy Mater. Sol. Cells.,* **2021**, *231*, 111329.

[24] Yin, X.; Zhang, Y.; Xu, X.; Wang, Y., Bilayer fiber membrane electrospun from MOF derived Co3S4 and PAN for solar steam generation induced sea water desalination. *J. Solid State Chem.,* **2021**, *303*, 122423.

[25] Lu, Y.; Fan, D.; Shen, Z.; Zhang, H.; Xu, H.; Yang, X., Design and performance boost of a MOF-functionalized-wood solar evaporator through tuning the hydrogen-bonding interactions. *Nano Energy.,* **2022**, *95*, 107016.

[26] Ma, X.; Li, Z.; Deng, Z.; Chen, D.; Wang, X.; Wan, X.; Fang, Z.; Peng, X., Efficiently cogenerating drinkable water and electricity from seawater via flexible MOF nanorod arrays. *J. Mater. Chem. A,* **2021**, *9*, 9048-9055.

[27] Saad, A. G.; Gebreil, A.; Kospa, D. A.; El-Hakam, S. A.; Ibrahim, A. A., Integrated solar seawater desalination and power generation via plasmonic sawdust-derived biochar: Waste to wealth. *Desalination.,* **2022**, *535*, 115824.

[28] Zhang, P.; Li, J.; Lv, L.; Zhao, Y.; Qu, L., Vertically Aligned Graphene Sheets Membrane for Highly Efficient Solar Thermal Generation of Clean Water. *ACS nano.,* **2017**, *11*, 5087-5093.

[29] Sun, Z.; Wang, J.; Wu, Q.; Wang, Z.; Wang, Z.; Sun, J.; Liu, C. J., Plasmon Based Double-Layer Hydrogel Device for a Highly Efficient Solar Vapor Generation. *Adv. Funct. Mater*., **2019**, *29*, 1901312.

[30] Wang, X.; Li, X.; Liu, G.; Li, J.; Hu, X.; Xu, N.; Zhao, W.; Zhu, B.; Zhu, J., An Interfacial Solar Heating Assisted Liquid Sorbent Atmospheric Water Generator. *Angew. Chem. Int. Ed.,* **2019**, *58*, 12054-12058.